Excitation Functions for Spallation Products and Fission Isomers in ^{237}Np(^{4}He, xn)$^{241-x}$Am Reactions*

Alain Fleury

*Department of Chemistry, State University of New York at Stony Brook, Stony Brook, New York 11790,
Centre d'Etudes Nucléaires de Bordeaux-Gradignan, Gradignan, France*

and

F. H. Ruddy,† M. N. Namboodiri,‡ and John M. Alexander

Department of Chemistry, State University of New York at Stony Brook, Stony Brook, New York 11790

Cross sections as a function of energy (19–46 MeV) have been measured for the following products from the reactions of ^{4}He with ^{237}Np: ^{237g}Am, ^{238g}Am, ^{238m}Am, ^{239g}Am, ^{239m}Am, ^{240g}Am. The prompt fission and total reaction cross sections have also been determined from 19 to 23 MeV. Isomer ratios as a function of excitation energy are presented for several fission isomers.

I. INTRODUCTION

Recently, the detailed energy dependence of fission isomer cross sections has been investigated by a number of workers.[1-4] Attempts have been made[2,5] to describe these excitation functions by statistical model calculations which include the presence of a double-humped fission barrier with nuclear states in greatly deformed "second-well" configurations. However, the comparison of theory and experiment suffers from the paucity of excitation-function measurements for spallation products in the ground state. A previous study[6] of the present reaction system, ^{237}Np + ^{4}He, and most of the studies of these heavy-mass spallation products in general[7] were made some years ago using cyclotron beams with questionable energy definition. The present reaction system was chosen because cross sections could be determined conveniently for both the fission isomers and also the spallation products in the ground state.

II. EXPERIMENTAL DETAILS

Targets of ^{237}Np ($\simeq$100 μg/cm^2 of the oxide) were prepared by vacuum deposition onto aluminum backing foils.[8] These targets were suitable for observation of fission isomers by recoil techniques. Other targets were prepared by electroplating Np onto nickel; these were suitable for radiochemical cross-section measurements. Target thicknesses were measured by counting α particles from ^{237}Np with a Si(Li) surface-barrier detector. The effective target thickness for isomer cross sections was taken as $\simeq$56 μg/cm^2. (See Ref. 3 for details.)

Bombardments were carried out on the Brook-haven National Laboratory (BNL) 60-in. sector-focused cyclotron and on the Stony Brook model FN tandem Van de Graaff accelerator. The beam energies from the cyclotron were calibrated against the Van de Graaff by measuring the pulse heights from scattered beam particles. We used a Si(Li) surface-barrier detector mounted at 45° (lab) to a Au target foil (200 μg/cm^2).

In all bombardments, the integrated beam current was determined by measurement of ^{65}Zn produced in natural copper foils of 7 mg/cm^2. The ^{65}Zn excitation function (previously measured from the Coulomb barrier to $\simeq$35 MeV)[9] was extended to 46 MeV in a separate set of measurements at the BNL cyclotron.

For the fission isomer measurements plastic detectors were used to measure fission tracks as described in detail elsewhere.[3,4,10-12] The experimental arrangement is shown in Fig. 1 of Ref. 3. In brief, a thin plastic (Makrofol, 0.72-mg/cm^2) sheet was mounted perpendicular to the beam very nearly in the same plane as the target layer. A recoil catcher was placed at a distance greater than 12.5 cm from the target; the position had essentially no effect on the shape of the radial track distributions. The half-life of ^{239m}Am was determined from the radial distributions of tracks to be 200±80 nsec, in agreement with the values determined by previous workers.[1,2,13,14]

Radiochemical measurements were performed using a stacked-foil technique with nickel-backed neptunium targets interspersed between nickel catcher and degrader foils. The beam energy for each target was calculated from the incident energy and the energy loss compilation of Northcliffe and Schilling.[15] Near threshold the stack consisted of two targets and the energy degradation was

only $\simeq 2$ MeV. After bombardment the targets and backings were dissolved in 6 N HNO$_3$ and added to a column of AG 1X10 anion-exchange resin to remove nickel activities. Americium in the eluate was coprecipitated on La(OH)$_3$ in the presence of Zr holdback carrier, reprecipitated as LaF$_3$, and precipitated again as La(OH)$_3$. The resulting precipitate was dissolved in a minimum of saturated HCl solution and added to a Dowex-50X12 column which was then eluted with concentrated HCl. The americium band was collected and evaporated to dryness on a hot platinum foil.[16] The final sample was subsequently analyzed by γ-ray spectrometry. Chemical yields were determined to be 40-50% by spiking with [241]Am. The entire separation took approximately two hours; all sample spectra were essentially free of fission product, plutonium, or neptunium activities. The γ rays of interest and their abundances[17-19] are shown in Table I.

The prompt-fission cross section was measured as a function of energy by counting fission tracks registered in mica placed at 175° to the beam. A 25% correction was applied at all energies for anisotropy in the angular distribution of the fission products.[7]

III. RESULTS AND DISCUSSION

In Table II and Fig. 1 we give the measured values of the cross section for prompt fission and for
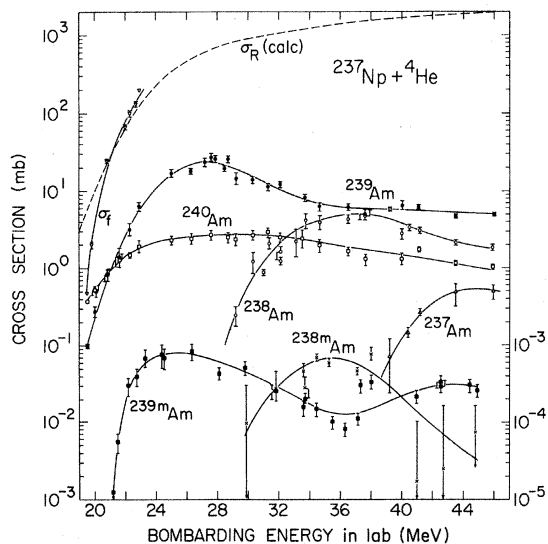

FIG. 1. Cross sections as a function of energy for products from the bombardment of [237]Np with 19–45-MeV helium ions. The symbols are as follows: $\triangledown$, fission cross section; $\square$, [240]Am; $\bullet$, [239]Am; $\blacksquare$, [239m]Am; $\bigcirc$, [238]Am; $\times$, [238m]Am; $\triangle$, [237]Am. The solid lines are drawn by eye through the points. The dashed line for σ_R was calculated from the optical model. Only relative values are given for [237]Am.

the production of [240]Am, [239]Am, [238]Am, and [237]Am. The total reaction cross section can be obtained by summing these cross sections. Of course the reactions involving charged particle emission are omitted in this sum, but this omission is not expected to be serious for energies less than 23 MeV. The ([4]He, n) reaction dominates for energies less than 21 MeV. At higher energies the ([4]He, 2n) reaction peaks at $\simeq 25$ mb followed by ([4]He, 3n) at $\simeq 5$ mb and then ([4]He, 4n). This well-known pattern reflects the very strong fission competition in the excited Am nuclei.[7]

Also given in Table II are optical-model calculations[20] of the total reaction cross section. Note that our measurement of the cross-section sum is significantly smaller than the calculation for 19.5 MeV. This difference is very important to the shape of the excitation function for ([4]He, 2n) as shown in Fig. 2 later. Presumably the optical-model calculations are reasonably accurate for energies greater than 23 MeV. However, this rather strong discrepancy near the Coulomb barrier should certainly be verified. It implies that the widely used optical-model calculations may not be useful near the Coulomb barrier.

Table III gives cross sections for the fission isomer [239m]Am and the ratio of cross sections for the isomers [238m]Am and [239m]Am. The stacked-detector technique used for measurement of this ratio is described in the Appendix. In brief, the second detector foil in a stack has much greater efficiency for 35-μsec [238m]Am[21, 22] than for 200-nsec [239m]Am. This difference in detection efficiencies allows the determination of the ratio of cross sections from the ratio of tracks in the two stacked foils.

The cross sections for reactions leading to the ground state and to the isomeric state have been divided by the total reaction cross section and plotted in Fig. 2. For energies near the threshold for the ([4]He, 2n) reaction (≤ 22 MeV) this fractional cross section increases abruptly (owing to the very steep decrease in the fission cross section near the barrier). If calculated total reaction cross sections are used rather than the experimental cross sections, this abrupt inflection disappears. The detailed characterization of the competition between fission and neutron emission requires that this situation be clarified. If the inflection is real it could result from a fission barrier greater than the neutron binding energy in [240]Am.

Figure 2 also shows that the excitation function for the isomer [239m]Am commences at a higher energy and increases to a maximum much more rapidly than that for the ground state. The apparent threshold is 2.5 ± 0.2 MeV greater than that for the ground state. The excitation function for the iso-

TABLE I. Properties of nuclides used in cross-section determinations.

Isotope	Half-life (h)	Photopeak energy (keV)	Number per disintegration	Reference
^{240}Am	51	1000	0.77	17
^{239}Am	12.1	226.4 + 228.2 [a]	0.146	18
		277.6	0.150	
^{238}Am	1.63	928	0.34	17, 19
		980	0.42	
^{237}Am	1.3	280.3	1 [b]	18

[a] Both γ rays were included in a single unresolved peak.
[b] The absolute value is not known; therefore only relative values of the cross sections can be reported.

TABLE II. Cross sections for reactions of ^{237}Np with ^{4}He (mb).

Bombarding energy (MeV) (lab)	(^{4}He, f)	(^{4}He, n)	(^{4}He, $2n$)	(^{4}He, $3n$)	(^{4}He, $4n$) [a]	$\sum_{1}^{4}\sigma_{xn}$	σ_R Measured	σ_R ABACUS [b]
19.5	0.466	0.372	0.097			0.469	0.935	5.4
19.8	2.02							
20.0		0.517	0.278			0.795	4.5	9.4
20.1		0.514						
20.8	24.0	0.823	0.837			1.66	25.66	22
21.6		1.28	1.43			2.71	52.7	47
22.0	66.4							65
22.3	101	1.48	3.26			4.74	106	80
22.7	133							
22.9	200	1.96	6.43			8.39	208	125
25.0		2.32	17.2			19.5		340
26.3		2.43	18.1			20.5		490
27.2			24.0					610
27.6		2.73	27.5			30.2		670
27.9			26.6					700
28.5			19.8					770
28.7		2.53	26.5					790
29.2		2.34	14.7	0.245		17.2		850
30.3		2.72	14.0	1.25		17.4		910
31.0				0.895				1020
31.3		2.91	11.3	2.08		15.3		1050
32.1				1.23				
32.1		2.50	12.2	1.62		15.6		1120
33.1				2.26				1210
33.7		2.45	8.20	4.25		12.89		1250
34.6		1.95	6.30	3.98		10.34		1310
36.5		1.64	6.16	4.41		10.12		1440
37.6		1.27	5.97	4.88		9.81		1510
39.2				5.37	0.072			1600
40.0		1.33	6.59	2.74				1640
40.4				3.31	0.148			1680
41.1		1.79	6.24	3.07	0.269	9.85		1700
43.5		1.17	4.82	2.13	0.481	7.59		1800
45.9		1.06	5.04	1.83	0.496	7.56		1910

[a] Relative values only; see Table I.
[b] Real well depth 50 MeV. Imaginary well depth 27 MeV. Interaction radius $1.17A^{1/3} + 1.77$ fm. Well difuseness 0.576 fm.

mer peaks at a lower energy and is significantly more narrow than that for the ground state. The rather high apparent cross sections for ^{239m}Am at bombarding energies greater than about 37 MeV may be due to contributions from other rather long-lived fission isomers, e.g. 82-nsec ^{237m1}Pu and 1120-nsec ^{237m2}Pu from the $(\alpha, p3n)$ reactions.[23] The data of Britt et al. indicate a peak cross section almost 1.7 times as large as we observe and a peak energy about 1 MeV larger. Interference from the $(^4\text{He}, n)$ reaction is more pronounced in their work, but this does not provide an explanation for the discrepancy.

The $(^4\text{He}, 3n)$ cross sections are also shown in Fig. 2. Again the excitation function for the isomer seems to have a smaller peak energy and seems to be more narrow than that for the ground state. The cross sections for ^{238m}Am have much greater uncertainties than those for ^{239m}Am because the stacked-detector technique was required. (See the Appendix.) At higher energies ($\geqslant$39 MeV) the presence of 5 nsec ^{237m}Am[22] formed via the $(\alpha, 4n)$ reaction could contribute tracks to detector 1. Decay curve analysis gives a limit of less than 10% of the events for the 5-nsec ^{237m}Am at an energy of 44.89 MeV. This limit corresponds to a maximum cross section of 30 nb.

The isomer ratios for several $(^4\text{He}, 2n)$ and $(^4\text{He}, 3n)$ reactions are plotted as a function of energy in Fig. 3.[2,3,22-31] The cross-section data for ground-state products limit the precision of these isomer ratios and the number of reactions for which they can be estimated. We have used smooth curves drawn in a systematic way through measured cross sections. The shapes of the isomer
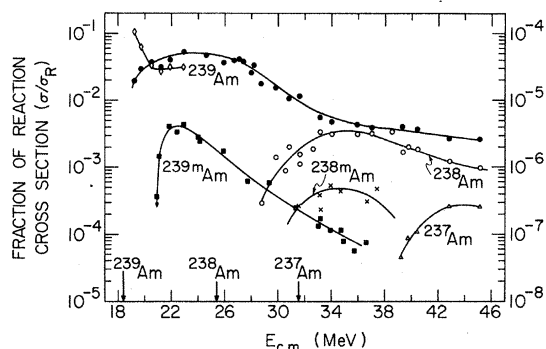
ratio curves seem to be well established. The maximum isomer ratios may well be uncertain by about a factor of 2 due to errors in absolute efficiencies etc. The isomer-ratio curves for $(^4\text{He}, 2n)$ reactions have a sharp peak and then decrease rather rapidly with increasing excitation energy. The curves for $(^4\text{He}, 3n)$ reactions are not so well determined but they appear to exhibit similar behavior. At the higher energies only upper limits are known for the cross sections for $(^4\text{He}, 3n)$ reactions due to the presence of interfering activities.

Maximum values of the isomer ratio (σ_i/σ_g) and full widths at half maximum for the isomer-ratio curves are summarized in Table IV. Previous[2,29] estimates of these ratios differ significantly from the values here, presumably due to differences in estimates of σ_g. A maximum isomer ratio of $\simeq 3 \times 10^{-4}$ with width 3 to 6 MeV appears to be typical of these reactions. These quantities should be very sensitive to changes in the fission-barrier parameters. In view of this expected sensitivity it is surprising that a number of these species have very similar maximum isomer ratios (4 ± 3) $\times 10^{-4}$ for $^{235,237-240}$Pu, $^{238-239}$Am, and $^{241-243}$Cm.[31] The maximum ratios are significantly smaller for

FIG. 2. Cross sections divided by total reaction cross section (σ/σ_R) as a function of energy in the c.m. system. The left scale is for ground states, the right for isomers. The symbols are the same as in Fig. 1. Values of σ_R were calculated from the optical model. For the $(^4\text{He}, 2n)$ reaction the experimental values of σ_R were also employed; the symbols used here are diamonds, $\Diamond$. Only relative values are given for ^{237}Am.

TABLE III. Cross sections for the fission isomers ^{238m}Am and ^{239m}Am.

Beam energy (lab) (MeV)	^{239m}Am (nb)	Cross-section ratio, $\sigma^{238m}/\sigma^{239m}$
21.24	<16	
21.44	73	
22.18	379	
22.74	482	
23.30	823	
24.38	870	
24.48	802	
26.31	974	
28.12	502	
29.81	598	0.18
31.83	299	1.06
33.61	183	2.92
33.71	238	1.36
34.44	171	4.56
35.25	181	3.77
35.44	121	
36.34	93	
37.17	<177	4.22
37.24	<359	
38.01	<391	2.23
40.96	<246	0.080
42.75	<385	0.086
42.75	<334	
44.43	<354	
44.89 [a]	<304	0.24

[a] A limit of less than 30 nb was calculated for the formation cross section of 5-nsec ^{237}Am at 44.89 MeV.

^{237}Am ($<0.6\times10^{-4}$) and ^{244}Cm (0.07×10^{-4}). The possibility exists, of course, that undetected isomers may correspond to the ground states of the second minimum for these cases. Also the very low value of (σ_i/σ_g) for ^{244}Cm may well be due, in part, to uncertainties in σ_g; the values of σ_g are quite large when compared to others in this region.

The similarity of the maximum isomer ratios and the similarity of the isomer-ratio curves points toward a strong similarity in the ratios of open channels to: (a) fission, (b) second-well states, and (c) first-well states. Such similarity demands either very similar second-well depths or rather few available states in the second well.

One may account for this pattern qualitatively in terms of the shape of the fission barriers. This is the approach of Jagare[5] and Britt et al.,[2] in their statistical model calculations. The double-humped barrier is assumed to exist in the product nucleus A and also in its precursor $A+1$. Excited states in either well of the $A+1$ nucleus can decay by neutron emission to the product A or may be lost by fission. The loss to fission must be more probable for states in the second well, as the fission barrier for the second well is not as high or broad as that for the first. Thus, as excitation energy increases, more of the population of excited states in the second well may be lost to fission and the isomer ratio may decrease with energy.

Alternatively, there may be only a small number of states in the second well of the product A that are capable of γ decay to the observed isomers. The precursor nucleus $A+1$ may not have any second-well states in the energy range of 9–14 MeV, and the concept of level density at the second barrier may not obtain.[32] Neutron emission may occur from any $A+1$ nucleus as it deforms toward fission. The probability of decay to the product nucleus A in the first or second well would then depend on the number of open channels to the A nucleus, independent of "trapping" in the second well of the parent $A+1$. In this situation, increasing the energy of the compound system could continue to open more decay channels to the first well after the few second well channels are all open. In this way the isomer ratio could reach a maximum and then decrease with increasing energy.

The objective of other work[33] in this laboratory is to use the GROGI 2 nuclear-evaporation program to calculate these excitation functions with the two above alternatives. A more detailed analysis of the experimental results awaits the model calculations.

TABLE IV. Maximum isomer ratios (σ_i/σ_g) for fission isomers produced in helium-ion bombardments.

Reaction	10^4 (σ_i/σ_g)	FWHM for isomer ratio curve	Reference
^{233}U(^{4}He, $2n$)^{235m}Pu	7	3.5	2, 25
^{235}U(^{4}He, $2n$)$^{237m1, m2}$Pu	4 [a]	5.0	2, 23, 25
^{236}U(^{4}He, $2n$)^{238m2}Pu	≈0.4 [b]	...	2, 24, 27, 28
^{236}U(^{4}He, $2n$)^{238m1}Pu	≈3 [b]	...	24–28
^{238}U(^{4}He, $2n$)^{240m}Pu	3	5.5	3, 24
^{238}U(^{4}He, $3n$)^{239m}Pu	3	...	3, 24
^{238}U(^{4}He, $4n$)^{238m2}Pu	<0.5	...	3, 24
^{238}U(^{4}He, $4n$)^{238m1}Pu	<20	...	3, 24
^{237}Np(^{4}He, $2n$)^{239m}Am	1.2	4.0	This work
	2	...	2, this work
^{237}Np(^{4}He, $3n$)^{238m}Am	1.8	...	This work
^{237}Np(^{4}He, $4n$)^{237m}Am	<0.6	...	This work
^{239}Pu(^{4}He, $2n$)^{241}Cm	1	4.5	2, 30
^{240}Pu(^{4}He, $2n$)^{242m}Cm	1	...	2, 30
^{242}Pu(^{4}He, $2n$)^{244m}Cm	0.07 [c]	...	2, 30
^{242}Pu(^{4}He, $3n$)^{243m}Cm	0.2 to 1	...	29, 30

[a] The measured isomer cross section is the sum of the cross sections for the two fission isomers of ^{237}Pu.

[b] The peak ratio of isomer to prompt fission was multiplied by an optical-model total reaction cross section and divided by a peak ground-state cross section calculated from available U(^{4}He, xn) data and Γ_F/Γ_T systematics.

[c] The value of σ_g from Ref. 30 seems very large compared to others in this region; this ratio may therefore be in error by even as much as an order of magnitude.
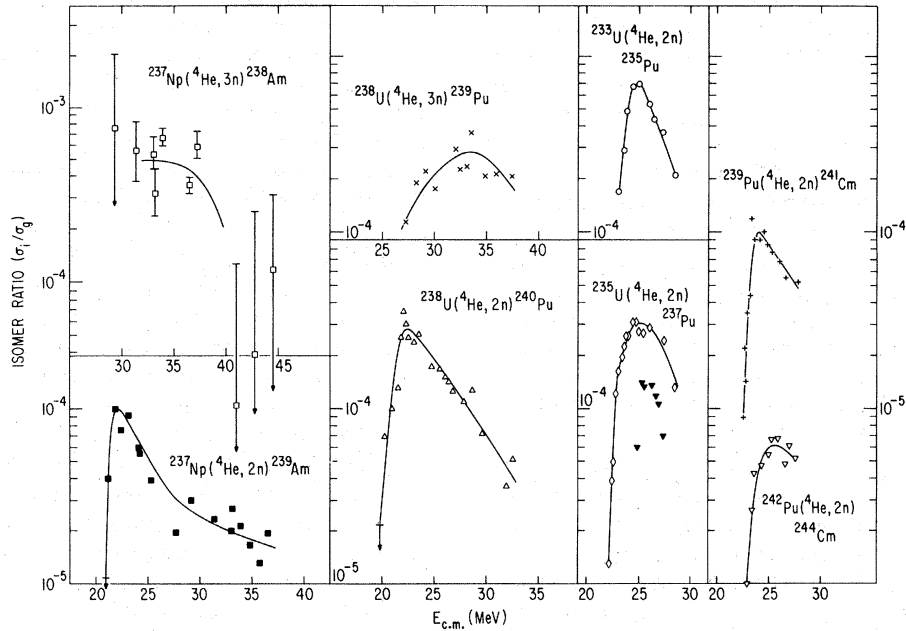
FIG. 3. Isomer ratios plotted as a function of energy in the c.m. system. Data are from the references given in Table IV. For production of ^{237}Pu the references are as follows: ▼, Ref. 23 (relative values only); ◇, Ref. 2.

APPENDIX. MEASUREMENT OF CROSS SECTION RATIOS OF 35-μsec ^{238m}Am TO 200-nsec ^{239m}Am

The cross section ratio for the fission isomers ^{238m}Am and ^{239m}Am was measured by use of a detector stack. The efficiency for detection is a strong function of the minimum dip angle of a fission fragment.[11] The minimum dip angle increases as the detector thickness increases; thus, in a stack of detectors the bottom layers will preferentially detect fission fragments which enter the detector with large dip angles. In order to resolve 200-nsec ^{239m}Am from 35-μsec ^{238m}Am, track detector thicknesses were chosen so that the second plastic layer would detect mainly events which originate from the recoil catcher. Most recoils of 35-μsec ^{238m}Am reach the catcher before decaying, whereas most recoils of 200-nsec ^{239m}Am decay in flight. The first plastic layer was thin enough (0.72 mg/cm^2) to detect both ^{239m}Am and ^{238m}Am. The total thickness for the first and second detectors was generally 1.89 mg/cm^2. For fission isomers produced with cross section σ and detected with efficiency ϵ, the ratio $R_{2/1}$ of number of events in the second detector (detector 2) to the number of events in the outermost layer (detector 1) is given by

$$R_{2/1} = \frac{\epsilon_2^{239}\sigma^{239} + \epsilon_2^{238}\sigma^{238}}{\epsilon_1^{239}\sigma^{239} + \epsilon_1^{238}\sigma^{238}},$$

where the superscripts refer to mass number and the subscripts to the detector. We assume that ^{238}Am is detected with the same efficiency in both detectors ($\epsilon_1^{238} = \epsilon_2^{238}$). (The fission fragments originate from the catcher and then have large enough dip angles for registration on both detectors.) The ratio of production cross sections is then given by

$$\frac{\sigma^{238}}{\sigma^{239}} = \frac{\epsilon_1^{239}(R_{2/1} - \epsilon_2^{239}/\epsilon_1^{239})}{\epsilon_1^{238}(1 - R_{2/1})}.$$

The quantities ϵ_1^{239} and ϵ_1^{238} have been calculated as described in Refs. 4 and 11. The quantity ϵ_2^{239} is not easily calculated, however. At or below the threshold for ^{238m}Am the ratio of detection efficiencies may be equated to the observed ratio of tracks $(R_{2/1})_0$,

$$(R_{2/1})_0 = \epsilon_2^{239}/\epsilon_1^{239},$$

and this experimental quantity may be used for conversion of the track ratios of Table III to cross-section ratios. [The contribution of (^{4}He,n) products is minimal.] An average value (0.047) for three experiments below threshold and two at high energy was used to calculate the points in Fig. 3. The error bars correspond to the extremes of the observed ratio $(R_{2/1})_0$ (0.012 and 0.068). The peak cross-section ratios are rather insensitive to $(R_{2/1})_0$, whereas the values for lower and higher energies are very sensitive to $(R_{2/1})_0$; they are

thus determined much less accurately.

The excitation function for ^{239m}Am was corrected for the presence of ^{238m}Am. The correction factor

for the total number of tracks observed is

$$1 - \frac{\epsilon_1^{238}(\sigma^{238}\sigma^{239})}{\epsilon_1^{239} + \epsilon_1^{238}(\sigma^{238}/\sigma^{239})}.$$

[1]S. C. Burnett, H. C. Britt, B. H. Erkkila, and W. E. Stein, Phys. Letters 31B, 523 (1970).

[2]H. C. Britt, S. C. Burnett, B. H. Erkkila, J. E. Lynn, and W. E. Stein, Phys. Rev. C 4, 1444 (1971). Figures presented here unify the measurements from earlier work.

[3]M. N. Namboodiri, F. H. Ruddy, and J. M. Alexander, preceding paper, Phys. Rev. C 7, 1222 (1973).

[4]M. N. Namboodiri, Ph.D. thesis, State University of New York at Stony Brook, 1972 (unpublished).

[5]S. Jagäre, Phys. Letters 32B, 571 (1970); Nucl. Phys. A137, 241 (1969).

[6]W. M. Gibson, University of California Radiation Laboratory Report No. UCRL-3493, 1956 (unpublished); R. M. Lessler, W. M. Gibson, and R. A. Glass, Nucl. Phys. 81, 401 (1966).

[7]E. K. Hyde, The Nuclear Properties of the Heavy Elements III. Fission Phenomena (Prentice Hall, Englewood Cliffs, N. J., 1964).

[8]Supplied by Oak Ridge National Laboratory, Oak Ridge, Tennessee.

[9]F. H. Ruddy, Ph.D. thesis, Department of Chemistry, Simon Fraser University, 1968 (unpublished).

[10]F. H. Ruddy, M. N. Namboodiri, and J. M. Alexander, Phys. Rev. C 3, 972 (1971).

[11]M. N. Namboodiri, F. H. Ruddy, and J. M. Alexander, Detection Efficiency of Annular Geometry Used in Fission Isomer Studies [Nucl. Instr. Methods (to be published)].

[12]N. L. Lark, Nucl. Instr. Methods 67, 137 (1969).

[13]N. L. Lark, G. Sletten, J. Pedersen, and S. Bjørnholm, Nucl. Phys. A139, 481 (1969).

[14]H. C. Britt, B. H. Erkkila, and B. B. Back, Phys. Rev. C 3, 1090 (1972).

[15]L. C. Northcliffe and R. F. Schilling, Nucl. Data A7, 233 (1970).

[16]R. A. Penneman, The Radiochemistry of Am and Cm, Nuclear Science of the National Research Council Committee on Nuclear Science Report No. Series, NAS-NS 3006, 1960 (unpublished).

[17]C. M. Lederer, J. M. Hollander, and I. Perlman, Table of Isotopes (Wiley, New York, 1967), 6th ed.

[18]F. T. Porter, I. Ahmad, M. S. Freedman, R. F. Barnes, R. K. Sjoblom, F. Wagner, Jr., and P. R. Fields, Phys. Rev. C 5, 1738 (1972); I. Ahmad, R. F. Barnes, P. R. Fields, and R. K. Sjoblom, Bull. Am. Phys. Soc. 15, 46 (1970).

[19]G. C. Post and A. H. W. Aten, Jr., Radiochemica Acta 15, 205 (1971).

[20]Calculated by the ABACUS 2 program of Auerbach. [E. H. Auerbach, Brookhaven National Laboratory Report No. BNL 6562, 1962 (unpublished)].

[21]J. Borggreen, Y. P. Gangrskii, G. Sletten, and S. Bjørnholm, Phys. Letters 25, 402 (1967).

[22]S. M. Polikanov and G. Sletten, Nucl. Phys. A151, 656 (1970).

[23]P. A. Russo, R. Vandenbosch, M. Mehta, J. S. Termer, and K. L. Wolf, Phys. Rev. C 3, 1595 (1971).

[24]J. Wing, W. J. Ramler, A. L. Harkness, and J. R. Huizenga, Phys. Rev. 114, 163 (1959).

[25]R. Vandenbosch, T. D. Thomas, S. E. Vandenbosch, R. A. Glass, and G. T. Seaborg, Phys. Rev. 111, 1358 (1958).

[26]R. Vandenbosch and G. T. Seaborg, Phys. Rev. 110, 507 (1958).

[27]J. A. Coleman, University of California Report No. UCRL-8186, 1958 (unpublished).

[28]P. Limkilde and G. Sletten, in Proceedings of the European Conference on Nuclear Physics, Aix-en-Provence, France, July 1972.

[29]K. L. Wolf and J. P. Unik, Phys. Letters 38B, 405 (1972).

[30]R. A. Glass, R. J. Carr, J. W. Cobble, and G. T. Seaborg, Phys. Rev. 104, 434 (1956).

[31]In the case of ^{238}Pu, a short-lived 0.5-nsec isomer has been identified (Ref. 28) in addition to the previously observed 5-nsec species. The latter has been assigned to an excited state in the second well, while the 0.5-nsec isomer has been assigned as the ground state of the second well (Ref. 28). The peak isomer ratio for the 5-nsec isomer is low compared to the trend established by the ground state and the other isomers tabulated. The low values of the upper limit for the 5-nsec ^{238}Pu isomer from the $(\alpha, 4n)$ data of Namboodiri, Ruddy, and Alexander (Ref. 3) are consistent with this result.

[32]V. S. Ramamurthy, S. S. Kapoor, and S. K. Kataria, Phys. Rev. Letters 25, 386 (1970); L. G. Moretto, Nucl. Phys. A182, 641 (1972).

[33]E. R. Jones, III, M. Pickering, A. Fleury, and J. M. Alexander, private communication.